Shell-model description of the nucleus ^{132}Te

J. Sau* and K. Heyde
Laboratorium voor Kernfysica, Proeftuinstraat 86, B-9000 Gent, Belgium

R. Chéry
Institut de Physique Nucléaire and IN2P3, Université Claude Bernard, Lyon-1 43, Bd du 11 Novembre 1918-69622 Villeurbanne Cedex, France

(Received 4 December 1978, revised manuscript received 14 June 1979)

Microscopic proton two-particle neutron two-hole shell-model calculations have been performed for the nucleus $^{132}_{52}Te_{80}$. Evidence results for the existence of a weak-coupling pattern obtained by coupling nuclear low-lying levels in $^{134}_{52}Te_{82}$ and $^{130}_{50}Sn_{80}$. Electromagnetic properties for the most important low-lying levels in $^{132}_{52}Te_{80}$ are also calculated and compared with existing experimental data. The limitations of proton two-particle- (neutron two-hole-) core coupling calculations are also exhibited when proton and/or neutron number only deviates from closed shell configurations by a small (± 2) number.

[NUCLEAR STRUCTURE $^{132}_{52}Te_{80}$ shell-model 2p – 2h calculations, electromagnetic properties, $T_{1/2}$, comparison with 2p(2h)-core coupling macroscopic calculations.]

I. INTRODUCTION

Recent experimental studies have indicated[1,2] that, if both proton and/or neutron number deviate from a closed shell configuration by only a small number of nucleons (± 2, ± 4), the typical two-particle (-hole), four-particle (-hole) degrees of freedom can still be clearly observed and are not averaged completely into a collective excitation pattern. Thus, also in the $^{132}_{52}Te_{80}$ nucleus, typical proton two-particle and neutron two-hole configurations clearly stand out in the experimental level scheme[3-6] and resemblance with a vibrational-like spectrum is only very crude, although such calculations have been carried out before.[7,8] Therefore, and because the basic building blocks $^{134}_{52}Te_{82}$, $^{130}_{50}Sn_{80}$, and $^{132}_{51}Sb_{81}$ constituting the nucleus under study are experimentally well known,[9-12] we have tried to study the limits of a unified-model treatment where only proton two-particle-(neutron two-hole-) core coupled configurations are treated and all neutron (proton) excitations are averaged out. Experimental evidence for specific neutron hole configurations of the type $(2d_{3/2}^{-1}1h_{11/2}^{-1})$ and $(3s_{1/2}^{-1}1h_{11/2}^{-1})$ is definitely available through the occurrence of low-lying $J^\pi = 7^-$ and 5^- levels in $^{132}_{52}Te_{80}$. Also, the proton $(1g_{7/2})_{4^+,6^+}^2$ configurations clearly stand out in the experimental spectrum. In Sec. II, the nuclear Hamiltonian as well as the solution of the nuclear secular equation are discussed whereas in Sec. III, the necessary transition matrix elements are obtained. Finally, in Sec. IV, the experimental results are compared with the shell-model calculations where different approximations have been used. Also, comparison is made with proton two-particle-(neutron two-hole-) core coupling calculations in order to point out in a clear way the shortcomings of such calculations when performed near closed shell configurations.

II. NUCLEAR HAMILTONIAN

The Hamiltonian describing the $^{132}_{52}Te_{80}$ nucleus, when both proton and neutron excitations occur, can be denoted as

$$H = \sum_{\substack{\alpha \\ (\pi,\nu)}} \epsilon_a a_\alpha^\dagger a_\alpha + \sum_{\substack{\alpha,\beta,\gamma,\delta \\ (\pi,\nu)}} V_{\alpha\beta\gamma\delta}\, a_\alpha^\dagger a_\beta^\dagger a_\delta a_\gamma + \sum_{\substack{\alpha,\gamma(\pi) \\ \beta,\delta(\nu)}} V'_{\alpha\beta\gamma\delta}\, a_\alpha^\dagger a_\beta^\dagger a_\delta a_\gamma \,. \tag{2.1}$$

The basis configurations are specified by (see Appendix A)

$$|(h_1h_2)J_n(p_1p_2)J_p; JM\rangle \equiv [(A_{h_1}^\dagger A_{h_2}^\dagger)J_n(A_{p_1}^\dagger A_{p_2}^\dagger)J_p]JM|\tilde{0}\rangle N, \tag{2.2}$$

where $|\tilde{0}\rangle$ denotes the (50, 82) doubly-closed shell vacuum state. The diagonal term of (2.1) contributes, within the basis (2.2), the single-particle energy $E_{p_1}+E_{p_2}+E_{h_1}+E_{h_2}$, whereas the proton-proton and neu-

tron-neutron interactions give the following contribution:

$$\langle h_1' h_2') J_n'(p_1' p_2') J_p'; JM | V_{pp} + V_{nn} | (h_1 h_2) J_n (p_1 p_2) J_p; JM \rangle = [\langle p_1' p_2'; J_p M_p | V_{pp} | p_1 p_2; J_p M_p \rangle D(h_1' h_2', h_1 h_2; J_n)$$
$$+ \langle h_1' h_2'; J_n M_n | V_{nn} | h_1 h_2; J_n M_n \rangle D(p_1' p_2', p_1 p_2; J_p)]$$
$$\times \delta_{J_p J_p'} \delta_{J_n J_n'} NN', \tag{2.3}$$

with

$$D(ab, cd; J) \equiv \delta_{ac}\,\delta_{bd} - (-1)^{j_a + j_b - J} \delta_{ad}\,\delta_{bc}\ , \tag{2.4}$$

$$N \equiv [\,(1 + \delta_{p_1 p_2})(1 + \delta_{h_1 h_2})]^{-1/2}\ ,$$

and N' equal to N with primed indices.

In calculating the proton-particle–neutron-hole interaction matrix elements, the coupling scheme for particle-particle angular momentum coupling is better adapted to the basis (2.2) chosen than the particle-hole angular momentum coupling scheme. Therefore, we can write the third contribution in (2.1) as

$$V_{ph} = \sum_{\substack{\rho;\rho,\eta;\eta \\ J;M'}} U((p'p)(h'h);J') A_\rho^\dagger, A_\eta^\dagger, A_\eta A_\rho \begin{pmatrix} j_p' & j_p & J' \\ -m_p' & m_p & -M' \end{pmatrix} \begin{pmatrix} j_h' & j_h & J' \\ -m_h' & m_h & M' \end{pmatrix} (-1)^{j_p' - m_p' + j_h' - m_h' + J' - M'}\ , \tag{2.5}$$

where $U((p'p)(h'h);J')$ stands for the angular momentum coupled matrix element of V_{ph} [V_{ph}, the third component of Eq. (2.1)]. Here we use the coupling scheme $(p'p)J'$ and $(h'h)J'$, as defined by Eq. (2.5).

If we define the direct matrix element of V_{ph} within the configuration space (2.2) as

$$F(h_1' h_2' J_n', p_1' p_2' J_p'; h_1 h_2 J_n, p_1 p_2 J_p; J) \equiv \langle (h_1' h_2') J_n' (p_1' p_2') J_p'; JM | V_{ph} | (h_1 h_2) J_n (p_1 p_2) J_p; JM \rangle_{n.a.s.}$$

($n.a.s.$ ≡ non-antisymmetrized) one obtains after some Racah algebra (see also Appendix A)

$$F(h_1' h_2' J_n',\ p_1' p_2' J_p'; h_1 h_2 J_n, p_1 p_2 J_p; J) \equiv \hat{J}_p \hat{J}_p' \hat{J}_n \hat{J}_n' NN' \delta_{h_1 h_1'}\ \delta_{p_2 p_2'}$$
$$\times \sum_{J'} U((p_1' p_1)(h_2' h_2); J') \begin{Bmatrix} j_{h_2}' & J' & j_{h_2} \\ J_n & j_{h_1} & J_n' \end{Bmatrix} \begin{Bmatrix} J_p & J' & J_p' \\ J_n' & J & J_n \end{Bmatrix} \begin{Bmatrix} J_p & J' & J_p' \\ j_{p_1}' & j_{p_2} & j_{p_1} \end{Bmatrix}$$
$$\times (-1)^{j_{h_1} + J_p + J + J_n + J' + j_{p_1} + J_p' + j_{p_2} + j_{h_2}' + J_n'}\ . \tag{2.6}$$

Defining the matrix element where the ket side has been antisymmetrized as

$$F_a(h_1' h_2' J_n', p_1' p_2' J_p'; h_1 h_2 J_n, p_1 p_2 J_p; J) \equiv \langle (h_1' h_2') J_n' (p_1' p_2') J_p'; JM | V_{ph} | \overline{(h_1 h_2) J_n (p_1 p_2) J_p; JM} \rangle$$

(here, $|\overline{\ldots}\rangle$ denotes the antisymmetrized ket vector), one obtains

$$F_a(h_1' h_2' J_n', p_1' p_2' J_p'; h_1 h_2 J_n, p_1 p_2 J_p; J) \equiv F(\ldots) - (-1)^{j_{p_1} + j_{p_2} + J_p} F(p_1 \rightleftharpoons p_2) - (-1)^{j_{h_1} + j_{h_2} + J_n} F(h_1 \rightleftharpoons h_2)$$
$$+ (-1)^{j_{p_1} + j_{p_2} + j_{h_1} + j_{h_2} + J_p + J_n} F(p_1 \rightleftharpoons p_2, h_1 \rightleftharpoons h_2)\ . \tag{2.7}$$

Thus the total proton-particle–neutron-hole matrix element is obtained as

$$\langle (h_1' h_2') J_n' (p_1' p_2') J_p'; JM | V_{ph} | (h_1 h_2) J_n (p_1 p_2) J_p; JM \rangle = F_a(h_1' h_2' J_n', p_1' p_2' J_p'; h_1 h_2 J_n, p_1 p_2 J_p; J)$$
$$- (-1)^{j_{p_1}' + j_{p_2}' + J_p'} F_a(p_1' \rightleftharpoons p_2') - (-1)^{j_{h_1}' + j_{h_2}' + J_n'} F_a(h_1' \rightleftharpoons h_2')$$
$$+ (-1)^{j_{p_1}' + j_{p_2}' + j_{h_1}' + j_{h_2}' + J_p' + J_n'} F_a(p_1' \rightleftharpoons p_2',\ h_1' \rightleftharpoons h_2')\ . \tag{2.8}$$

As already mentioned, in using the representation of (2.5) for the particle-hole interaction, an important

numerical simplification results as compared with the usual particle-hole coupled representation of this interaction.

III. TRANSITION MATRIX ELEMENTS

If we call $\langle a\|\Omega_\lambda\|b\rangle$ the independent particle reduced matrix element for the electromagnetic multipole operator Ω_λ, we can calculate the full reduced matrix element between the initial state $|J_i M_i\rangle$ and a final state $|J_f M_f\rangle$ as,

$$\langle J_f\|\Omega_\lambda\|J_i\rangle = \sum_{\{i,f\}} c_i(h_1h_2J_n, p_1p_2J_p; J_i)c_f(h_1'h_2'J_n', p_1'p_2'J_p'; J_f)\langle f\|\Omega_\lambda\|i\rangle , \tag{3.1}$$

where $\langle f\|\Omega_\lambda\|i\rangle$ denotes the basic transition matrix element that can be further separated into a proton and neutron contribution and $c_i(\ldots)$, $c_f(\ldots)$ denote the expansion coefficients of the initial and final state, respectively, within the basis of Eq. (2.2). For the proton contribution, we find as the direct term contribution

$$\Omega_p(h_1'h_2'J_n', p_1'p_2'J_p', J_f; h_1h_2J_n, p_1p_2J_p, J_i) \equiv \hat{J}_p\hat{J}_p'\hat{J}_i\hat{J}_f(-1)^{J_n'+J_p'+J_f+j_{p_1}+j_{p_2}+J_p} NN'\langle p_2'\|\Omega_\lambda\|p_2\rangle$$
$$\times \begin{Bmatrix} J_p' & \lambda & J_p \\ J_i & J_n & J_f \end{Bmatrix} \begin{Bmatrix} j_{p_2}' & \lambda & j_{p_2} \\ J_p & j_{p_1} & J_p' \end{Bmatrix} \delta_{p_1p_1'}\delta_{J_nJ_n'} D(h_1'h_2', h_1h_2; J_n) \tag{3.2}$$

(see also Appendix B), and for the matrix element taking into account the antisymmetry in initial and final states,

$$\langle f\|\Omega_\lambda\|i\rangle_p = \Omega_p(\ldots) - (-1)^{j_{p_1}'+j_{p_2}'+J_p'}\Omega_p(p_1'\rightleftarrows p_2') - (-1)^{j_{p_1}+j_{p_1}+J_p}\Omega_p(p_1\rightleftarrows p_2)$$
$$+ (-1)^{j_{p_1}'+j_{p_2}'+j_{p_1}+j_{p_2}+J_p+J_p'}\Omega_p(p_1'\rightleftarrows p_2', p_1\rightleftarrows p_2) . \tag{3.3}$$

After similar calculations, one obtains for the neutron contribution

$$\Omega_n(h_1'h_2'J_n', p_1'p_2'J_p', J_f; h_1h_2J_n, p_1p_2J_p, J_i) \equiv \hat{J}_n\hat{J}_n'\hat{J}_i\hat{J}_f NN'\langle h_2\|\Omega_\lambda\|h_2'\rangle(-1)^{j_{h_2}'-j_{h_1}+\lambda+J_p+J_i}$$
$$+ \begin{Bmatrix} J_n' & \lambda & J_n \\ J_i & J_p & J_f \end{Bmatrix} \begin{Bmatrix} j_{h_2}' & \lambda & j_{h_2} \\ J_n & j_{h_1} & J_n' \end{Bmatrix} \delta_{h_1h_1'}\delta_{J_pJ_p'} D(p_1'p_2', p_1p_2; J_p) , \tag{3.4}$$

with a similar expression for the total neutron matrix element $\langle f\|\Omega_\lambda\|i\rangle_n$ as given in Eq. (3.3). The final matrix element then results by making use of the equation (3.1) and using

$$\langle f\|\Omega_\lambda\|i\rangle = \langle f\|\Omega_\lambda\|i\rangle_p + \langle f\|\Omega_\lambda\|i\rangle_n . \tag{3.5}$$

IV. RESULTS AND DISCUSSION

A. Energy spectra

In performing the calculations, based on Secs. II and III, the proton-proton as well as neutron-neutron interactions have been taken to be of Gaussian shape with spin exchange admixture, i.e., $V = V_0 e^{-\beta r^2}(P_S + tP_T)$, in line with studies of $N = 82$ and $N = 83$ nuclei within this particular mass region.[13-16] For the proton-neutron interaction on the other hand, an interaction of the form $V = V_1\delta(\vec{r}_p - \vec{r}_n)(P_S + t'P_T)$, as discussed in Sec. II and also used in the same mass region,[16,17] has been considered. Here, P_S and P_T denote the spin singlet and spin triplet projection operators. In the Gaussian interaction a value of $\beta = 0.325$ fm^{-2} was used throughout.

For this particular nucleus $^{132}_{52}\mathrm{Te}_{80}$, the separate p-p, n-n, and p-n interactions were determined by studying the adjacent nuclei $^{134}_{52}\mathrm{Te}_{82}$, $^{130}_{50}\mathrm{Sn}_{80}$, and $^{132}_{51}\mathrm{Sb}_{81}$ and searching for the best agreement with the experimental data. The parameters V_0, V_1, t, and t' as well as the proton and neutron single-particle (-hole) energies thus determined are given in Table I, and correspond to the experimental single-particle (-hole) energies as observed in $^{133}_{51}\mathrm{Sb}_{82}$ and $^{131}_{50}\mathrm{Sn}_{81}$, respectively.[18,19] In Figs. 1, 2, and 3, the calculated and experimental results for these three nuclei are given.[9-12]

Starting from the residual p-p, n-n, and p-n interactions as well as the proton and neutron single-particle (-hole) energies thus determined,

TABLE I. The parameters for the proton-proton, neutron-neutron, and proton-neutron interaction as well as the proton single-particle and neutron single-hole energies. Values for the small space (A) and the full configuration space (B) are given separately (see also Sec. IV). For the proton single-particle energies and full space (B), calculations with $E_{2d_{5/2}}=0.75$ MeV and $E_{1h_{11/2}}=3.0$ MeV have also been performed.

	Proton			Neutron	
	A	B		A	B
$E_{1g_{7/2}}$	0.0	0.0	$E_{2d_{3/2}}$	0.0	0.0
$E_{2d_{5/2}}$	1.0	1.0	$E_{3s_{1/2}}$	0.3	0.3
$E_{1h_{11/2}}$		2.0	$E_{1h_{11/2}}$	0.4	0.4
$E_{2d_{3/2}}$		2.4	$E_{1g_{7/2}}$		2.4
$E_{3s_{1/2}}$		2.0	$E_{2d_{5/2}}$		2.8
V_0	−50	−39	V_0	−50	−39
t	+ 0.2	+ 0.2	t	+ 0.2	+ 0.2
	$V_1=-84$ (MeV fm^3)				
	$t'=5$				

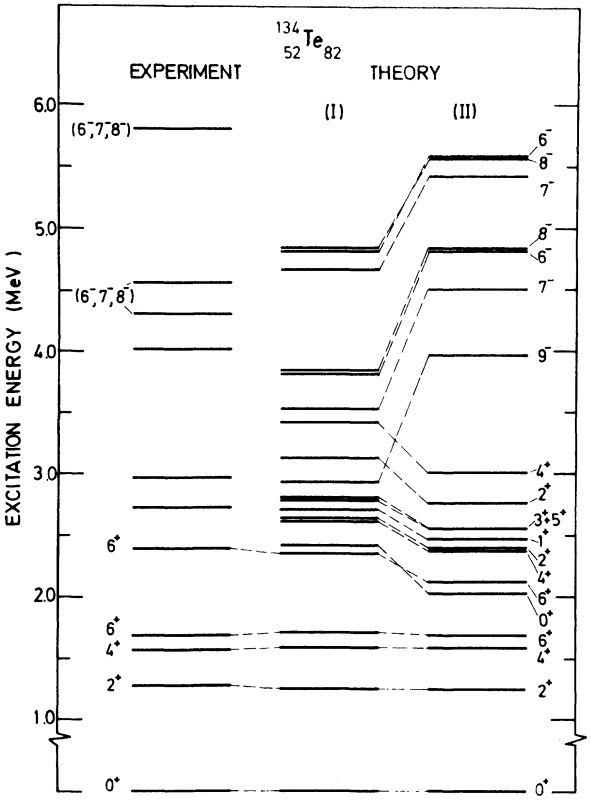

FIG. 1. Comparison for $^{134}_{52}Te_{82}$ between experimental data (Refs. 9 and 10) and theoretical results using the proton single-particle energies and force strength parameters of Table I (B) (calculation I). Also, the calculation with changes in the proton single-particle energies $E_{2d_{5/2}}=0.75$ MeV and $E_{1h_{11/2}}=3.0$ MeV have been performed (calculation II).

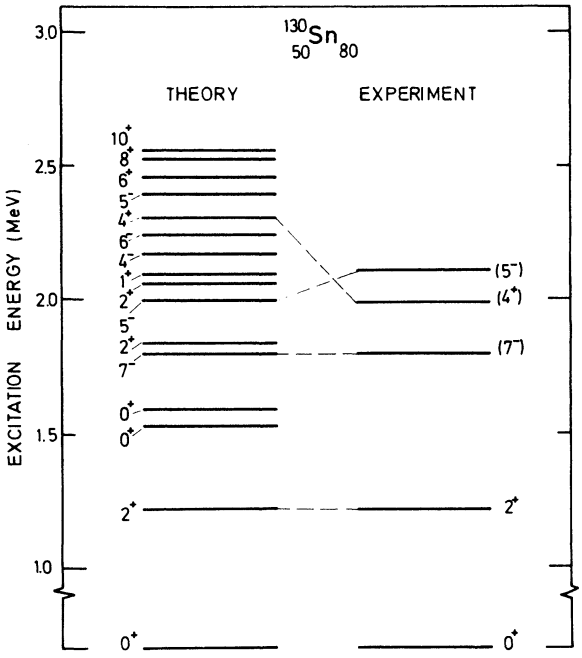

FIG. 2. Comparison for $^{130}_{50}Sn_{80}$ between experimental data (Ref. 5) and theoretical results using the neutron single-hole energies force strength parameters of Table I(B).

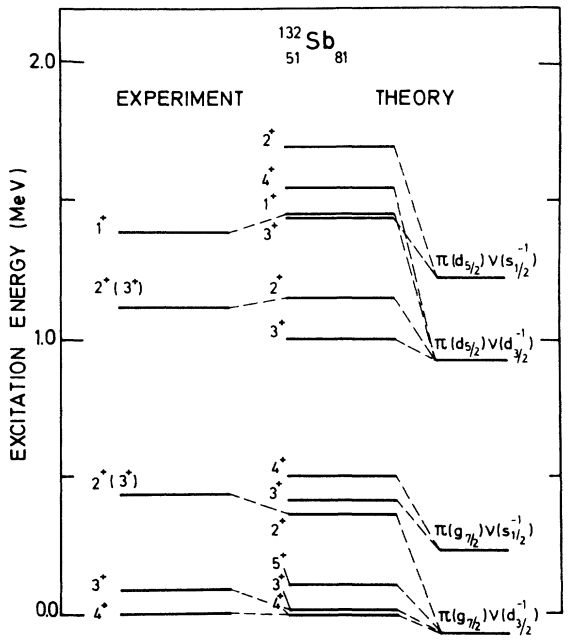

FIG. 3. Comparison for $^{132}_{51}Sb_{81}$ between experimental (Ref. 12) and theoretical results using single-particle (– hole) energies and force strength parameters of Table I (B). The unperturbed proton-neutron configurations are also drawn.

one can solve the secular equation corresponding to the Hamiltonian discussed in Sec. II and calculate transition rates, using the formulas of Sec. III. Already by studying the separate results for the proton two-particle and neutron two-hole nuclei in some detail, we expect, through the coupling of both subsystems by means of the δ proton-neutron interaction, to observe both proton and neutron excitations in a pronounced way in the final $^{132}_{52}Te_{80}$ nucleus.

In obtaining these final results, we also have made some approximations in truncating the configuration space available for both proton and neutron single-particle (-hole) configurations, to the most important ones. We used

(i) approximation (A): proton levels $1g_{7/2}$, $2d_{5/2}$ and neutron levels $2d_{3/2}^{-1}$, $3s_{1/2}^{-1}$, $1h_{11/2}^{-1}$,

(ii) full space (B): all proton and neutron levels in the 50–82 shell, i.e., $1g_{7/2}$, $2d_{5/2}$, $2d_{3/2}$, $3s_{1/2}$, and $1h_{11/2}$. One has to remark that in considering the full space, matrices of a typical dimension 1000×1000 occur and have been diagonalized. Moreover, because the force strength parameters, given in Table I(B), were determined for the complete configuration space for either protons (neutrons) separately, some renormalization in approximation (A) will have to be incorporated on force strengths in order to reach an overall agreement with the experimental data. These parameters [approx (A)] are also given in Table I.

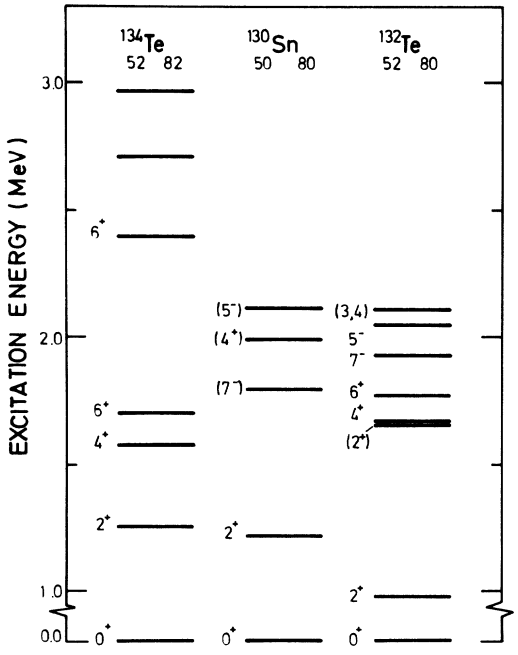

FIG. 4. The important low-lying levels in ^{134}Te, ^{130}Sn, and in the nucleus ^{132}Te, indicating the weak-coupling pattern.

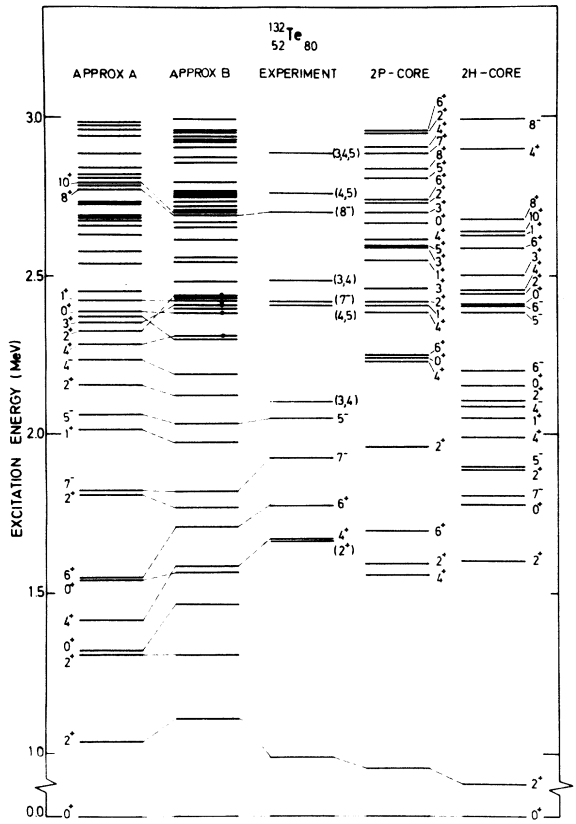

FIG. 5. Comparison of the experimental data in ^{132}Te (Refs. 3–6) with the microscopic proton two-particle neutron two-hole calculations within approximation (A) and using the full space (B). The results of unified-model calculations where, respectively, proton two-particle (or neutron two-hole) configurations are coupled to quadrupole vibrations of a core nucleus, are also given. Dashed lines connect levels with definite J^π assignment.

Before studying in detail the correspondence between calculated and experimental level schemes, one can very clearly distinguish a weak-coupling pattern in constructing states in $^{132}_{52}Te_{80}$, starting from the ^{134}Te and ^{130}Sn adjacent doubly-even nuclei (Fig. 4). The states in ^{132}Te with specific proton and neutron configurations stand out very clearly. A new level, recently found, at 1665.3 keV (Ref. 3) in ^{132}Te can very probably be associated with the $J_i^\pi = 2_2^+$ (or 2_3^+) theoretical level.

In comparing approximations (A) and (B) with experiment, up to $E_x = 2$ MeV, good overall agreement occurs although three extra low-lying levels $[J_i^\pi = 0_2^+, 0_3^+, 2_2^+ \text{ (or } 2_3^+)]$ result in the calculations (see Fig. 5). Above $E_x \simeq 2$ MeV, no detailed comparison is possible due to the growing density of proton two-particle coupled to neutron two-hole configurations. In studying the wave functions

corresponding with the $J_i^\pi = 0_1^+$, 2_1^+, 4_1^+, 6_1^+, 5_1^-, 7_1^-, 8_1^+, and 10_1^+ levels (see Table II), one immediately recognizes that in coupling the $^{134}_{52}Te_{82}$ and $^{130}_{50}Sn_{30}$ subsystems by means of the residual p-n interaction, a weak-coupling mechanism seems to be acting. Therefore, one can try a decomposition of the wave functions in a direct coupling representation.

TABLE II. Wave functions for the lowest-lying states in ^{132}Te as obtained in both approximation (A) (first column) and the full space (B) (second column). The 2h – 2p configurations are always indicated within the $(j_{h_1} j_{h_2})J_n$ $(j_{p_1} j_{p_2})J_p$ basis space. Excitation energies (MeV) are also indicated as the numbers between parentheses. A dash means that the corresponding amplitude squared (intensity) is less then 0.04. This criterion is also used to leave out (only in the table) the other configurations constituting the complete wave functions.

Configuration	(0.0)	0_1^+	(0.0)	(1.322)	0_2^+	(1.467)
$(2d_{3/2})_{0^+}^{-2}(1g_{7/2})_{0^+}^{2}$	0.68		0.62	0.43		0.36
$(3s_{1/2})_{0^+}^{-2}(1g_{7/2})_{0^+}^{2}$	0.51		0.39	−0.85		−0.82
$(1h_{11/2})_{0^+}^{-2}(1g_{7/2})_{0^+}^{2}$	−0.50		−0.47	−0.26		···
$(3s_{1/2})_{0^+}^{-2}(2d_{5/2})_{0^+}^{2}$	···		···	···		−0.22
$(3s_{1/2})_{0^+}^{-2}(1h_{11/2})_{0^+}^{2}$	···		···	···		0.24
	(1.038)	2_1^+	(1.109)	(1.307)	2_2^+	(1.306)
$(2d_{3/2})_{0^+}^{-2}(1g_{7/2})_{2^+}^{2}$	0.67		0.42	···		0.51
$(3s_{1/2})_{0^+}^{-2}(1g_{7/2})_{2^+}^{2}$	0.48		0.24	···		0.33
$(1h_{11/2})_{0^+}^{-2}(1g_{7/2})_{2^+}^{2}$	−0.47		−0.30	···		−0.37
$(1h_{11/2})_{2^+}^{-2}(1g_{7/2})_{0^+}^{2}$	···		0.22	−0.22		
$(2d_{3/2})_{2^+}^{-2}(1g_{7/2})_{0^+}^{2}$	−0.25		−0.49	0.59		0.27
$(2d_{3/2}^{-1}3s_{1/2}^{-1})_{2^+}(1g_{7/2})_{0^+}^{2}$	···		0.43	−0.73		−0.49
	(1.412)	4_1^+	(1.582)			
$(2d_{3/2})_{0^+}^{-2}(1g_{7/2})_{4^+}^{2}$	0.68		0.68			
$(3s_{1/2})_{0^+}^{-2}(1g_{7/2})_{4^+}^{2}$	0.52		0.42			
$(1h_{11/2})_{0^+}^{-2}(1g_{7/2})_{4^+}^{2}$	−0.49		−0.48			
	(1.547)	6_1^+	(1.705)			
$(2d_{3/2})_{0^+}^{-2}(1g_{7/2})_{6^+}^{2}$	0.68		0.68			
$(3s_{1/2})_{0^+}^{-2}(1g_{7/2})_{6^+}^{2}$	0.52		0.42			
$(1h_{11/2})_{0^+}^{-2}(1g_{7/2})_{6^+}^{2}$	−0.49		−0.48			
	(2.778)	8_1^+	(2.697)			
$(1h_{11/2})_{8^+}^{-2}(1g_{7/2})_{0^+}^{2}$	0.94		0.85			
$(1h_{11/2})_{8^+}^{-2}(2d_{5/2})_{0^+}^{2}$	···		0.31			
$(1h_{11/2})_{8^+}^{-2}(1h_{11/2})_{0^+}^{2}$	···		−0.26			
	(2.800)	10_1^+	(2.704)			
$(1h_{11/2})_{10^+}^{-2}(1g_{7/2})_{0^+}^{2}$	0.93		0.84			
$(1h_{11/2})_{10^+}^{-2}(2d_{5/2})_{0^+}^{2}$	···		0.31			
$(1h_{11/2})_{10^+}^{-2}(1h_{11/2})_{0^+}^{2}$	···		−0.26			
$(1h_{11/2})_{10^+}^{-2}(1g_{7/2})_{2^+}^{2}$	−0.28		−0.22			

TABLE II. *(Continued)*.

Configuration	(1.827)	7^-_1	(1.823)
$(2d_{3/2}^{-1}1h_{11/2}^{-1})_7 - (1g_{7/2})_{0^+}{}^2$	0.96		0.87
$(2d_{3/2}^{-1}1h_{11/2}^{-1})_7 - (1g_{7/2})_{2^+}{}^2$	−0.25		−0.20
$(2d_{3/2}^{-1}1h_{11/2}^{-1})_7 - (2d_{5/2})_{0^+}{}^2$	...		0.25
$(2d_{3/2}^{-1}1h_{11/2}^{-1})_7 - (1h_{11/2})_{0^+}{}^2$	...		−0.26
	(2.065)	5^-_1	(2.035)
$(2d_{3/2}^{-1}1h_{11/2}^{-1})_5 - (1g_{7/2})_{0^+}{}^2$	−0.72		−0.68
$(3s_{1/2}^{-1}1h_{11/2}^{-1})_5 - (1g_{7/2})_{0^+}{}^2$	0.65		0.56
$(2d_{3/2}^{-1}1h_{11/2}^{-1})_5 - (1h_{11/2})_{0^+}{}^2$	...		0.20

By means of diagonalizing within the proton space, the proton particle-particle interaction V_{pp} and, in the neutron space, the neutron hole-hole interaction V_{nn} (in both cases, all configurations in the 50–82 shell are considered) as well as directly diagonalizing within the full two-proton-particle–two-neutron-hole space [approx (B)], the total interaction $V_{pp}+V_{nn}+V_{ph}$, the wave functions

$$|J_n(\nu),k\rangle = \sum_{h_1,h_2} h^k(h_1h_2,J_n)|(h_1h_2)J_n\rangle\,, \tag{4.1}$$

$$|J_p(\pi),l\rangle = \sum_{p_1,p_2} p^l(p_1p_2,J_p)|(p_1p_2)J_p\rangle\,, \tag{4.2}$$

and

$$|J_i\rangle = \sum_{\substack{h_1,h_2,J_n\\ p_1,p_2,J_p}} c_i(h_1h_2J_n,\,p_1p_2J_p;J) \times|(h_1h_2)J_n(p_1p_2)J_p;J\rangle \tag{4.3}$$

in ^{130}Sn, ^{134}Te, and ^{132}Te are obtained. Inverting the relations (4.1) and (4.2), one can express the states (4.3) within the coupled basis of (4.1) and (4.2) as

$$|J_i\rangle = \sum_{\substack{J_n(\nu),J_p(\pi)\\ k,l}} a_i[J_n(\nu),k;J_p(\pi),l;J] \times|J_n(\nu)k\otimes J_p(\pi),l\rangle\,. \tag{4.4}$$

The wave functions (4.4) for some of the important low-lying levels in ^{132}Te, are shown in Table III. Here, the weak-coupling picture, at least for the lowest states, becomes immediately clear. The levels $J_i^\pi = 2_2^+$, 4_1^+, 6_1^+ are the proton excited $J_i^\pi = 2_1^+$, 4_1^+, and 6_1^+ states in ^{134}Te coupled to the ^{130}Sn $J^\pi = 0^+$ ground state, whereas the $J_i^\pi = 5_1^-$, 7_1^-, 8_1^+, and 10_1^+ are mainly the ^{130}Sn excited $J_i^\pi = 5_1^-$, 7_1^-, 8_1^+, and 10_1^+ states coupled to the ^{134}Te $J^\pi = 0^+$ ground state. The structure of the $J_i^\pi = 2_1^+$ level is mainly the neutron ^{130}Sn $J^\pi = 2^+$ first excited state coupled with the ^{134}Te $J^\pi = 0^+$ ground state. The multiplet $|2_1^+(\nu)\otimes 2_1^+(\pi)\rangle$ $(J^\pi = 0_4^+,\ 1_2^+,\ 2_5^+,\ 3_1^+,\ 4_2^+)$ is observed as a weak-coupling multiplet of states near the unperturbed energy of $E_x(2_1^+,\ ^{134}\text{Te}) + E_x(2_1^+,\ ^{130}\text{Sn}) = 2.478$ MeV.

B. Comparison with unified-model calculations

Within the unified-model type of calculations,[7,8,20,21] taking only explicitly into account

TABLE III. The wave functions for some of the low-lying levels of ^{132}Te, expressed in the basis (4.4). The same truncation as in Table II is used to limit the expansion of the wave functions as given in the table. The first column gives the theoretical excitation energy in MeV (approximation B only).

0.000	$\|0_1^+\rangle = -0.98\,\|0_1^+(\nu)\otimes 0_1^+(\pi)\rangle$
1.467	$\|0_2^+\rangle = 0.86\,\|0_3^+(\nu)\otimes 0_1^+(\pi)\rangle + 0.49\,\|0_2^+(\nu)\otimes 0_1^+(\pi)\rangle$
1.566	$\|0_3^+\rangle = 0.83\,\|0_2^+(\nu)\otimes 0_1^+(\pi)\rangle - 0.47\,\|0_3^+(\nu)\otimes 0_1^+(\pi)\rangle$
1.977	$\|1_1^+\rangle = 0.96\,\|1_1^+(\nu)\otimes 0_1^+(\pi)\rangle - 0.24\,\|2_1^+(\nu)\otimes 2_1^+(\pi)\rangle$
2.425	$\|1_2^+\rangle = 0.94\,\|2_1^+(\nu)\otimes 2_1^+(\pi)\rangle + 0.24\,\|1_1^+(\nu)\otimes 0_1^+(\pi)\rangle$
1.306	$\|2_2^+\rangle = 0.75\,\|0_1^+(\nu)\otimes 2_1^+(\pi)\rangle + 0.60\,\|2_1^+(\nu)\otimes 0_1^+(\pi)\rangle$
1.109	$\|2_1^+\rangle = -0.78\,\|2_1^+(\nu)\otimes 0_1^+(\pi)\rangle + 0.61\,\|0_1^+(\nu)\otimes 2_1^+(\pi)\rangle$
2.408	$\|3_1^+\rangle = 0.97\,\|2_1^+(\nu)\otimes 2_1^+(\pi)\rangle$
1.582	$\|4_1^+\rangle = 0.97\,\|0_1^+(\nu)\otimes 4_1^+(\pi)\rangle$
2.480	$\|4_3^+\rangle = 0.81\,\|4_1^+(\nu)\otimes 0_1^+(\pi)\rangle - 0.46\,\|2_1^+(\nu)\otimes 2_1^+(\pi)\rangle$
2.310	$\|4_2^+\rangle = 0.84\,\|2_1^+(\nu)\otimes 2_1^+(\pi)\rangle + 0.49\,\|4_1^+(\nu)\otimes 0_1^+(\pi)\rangle$
1.705	$\|6_1^+\rangle = 0.97\,\|0_1^+(\nu)\otimes 6_1^+(\pi)\rangle$
2.697	$\|8_1^+\rangle = 0.96\,\|8_1^+(\nu)\otimes 0_1^+(\pi)\rangle$
2.764	$\|8_2^+\rangle = 0.98\,\|2_1^+(\nu)\otimes 6_1^+(\pi)\rangle$
2.704	$\|10_1^+\rangle = 0.95\,\|10_1^+(\nu)\otimes 0_1^+(\pi)\rangle - 0.24\,\|10_1^+(\nu)\otimes 2_1^+(\pi)\rangle$
2.035	$\|5_1^-\rangle = 0.97\,\|5_1^-(\nu)\otimes 0_1^+(\pi)\rangle$
1.823	$\|7_1^-\rangle = 0.96\,\|7_1^-(\nu)\otimes 0_1^+(\pi)\rangle - 0.22\,\|7_1^-(\nu)\otimes 2_1^+(\pi)\rangle$

the proton two-particle (neutron two-hole) configurations coupled with the core excitations of the ^{130}Sn (^{134}Te) nucleus, important simplifications have to be made. Results from both types of macroscopic particle (-hole)-core coupling calculations are compared with each other and with the fully microscopic calculations in Fig. 5, thereby showing some of the apparent shortcomings in the unified-model calculations. Within the proton two-particle-core coupling calculations, the parameters of Ref. 7 have been used. No low-lying negative parity levels ($J^\pi = 5^-, 6^-, 7^-$) occur and also, a low-lying $J^\pi = 0^+$ state originating from neutron two-hole configurations is not reproduced.

For the neutron two-hole-core coupling calculation, the same neutron single-particle energies as discussed in Table I, full space (B), have been considered. The core was specified with $\hbar\omega_2$ equal to the experimental $J_i^\pi = 0_1^+$ to 2_1^+ energy separation in $^{134}_{52}\mathrm{Te}_{82}$, the residual neutron-neutron interaction was a surface delta interaction (SDI) force with force strength $G = 0.21$ MeV, whereas the hole-core coupling strength $\xi_2 = 1.0$ was taken, a value consistent with the experimental $B(E2; 2_1^+ \to 0_1^+)$ value in ^{134}Te. In this calculation, the low-lying $J^\pi = 4^+$ and 6^+ levels are missing as compared with experiment and with the fully microscopic approach.

C. Electromagnetic properties

Because only very few experimental transition rates are known, we have calculated the electromagnetic properties of some selected levels, such as the lifetime for the $J_i^\pi = 6_1^+$ level deexciting via an $E2$ transition towards the $J_i^\pi = 4_1^+$ level. In calculating transition rates, the effective charges $e_p = 1.5e$, $e_n = 0.5e$, $g_s^{\mathrm{eff}} = 0.5\, g_s^{\mathrm{free}}$ have been used throughout. In approximation (A), a value $T_{1/2}(6_1^+) = 257$ nsec [226 nsec in full space (B)] results, which is to be compared with the experimental value of 145 nsec. In trying to calculate the lifetime of the $J_i^\pi = 7_1^-$ level, deexciting towards the $J_i^\pi = 6_1^+$ level, within the model spaces (A) and (B), no $E1$ transitions can occur. The lowest multipolarity contributing in model space (A) is $M4$, whereas in the full space (B), $M2$ transitions can occur with $T_{1/2}(7_1^-) = 0.038$ sec. These results point towards a small but definite admixture of proton and/or neutron excitations out of, respectively, the $Z = 50$ proton and/or $N = 82$ neutron closed shell configuration, making $E1$ transitions possible. The $5_1^- \to 7_1^-$ $E2$ transition results in a value $T_{1/2}(5_1^-) = 0.21$ μsec in model space (A) [0.23 μsec in full space (B)].

A possible explanation for the recently observed $T_{1/2} = 3.9$ μsec isomeric state[6, 22] at 2.701 MeV

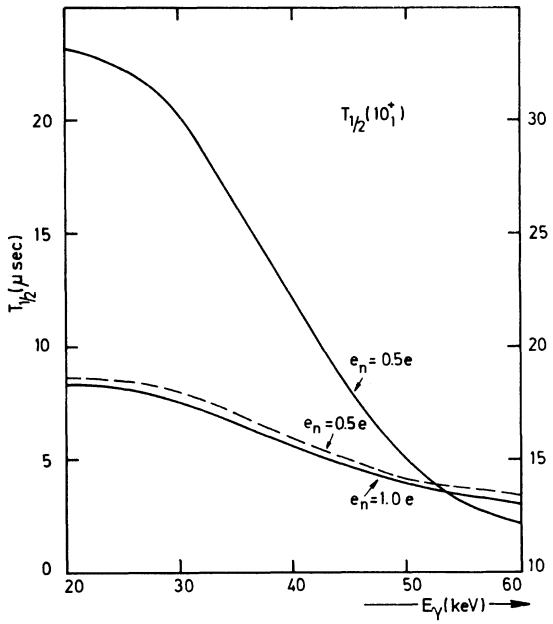

FIG. 6. Calculated half-life for the $J_i^\pi = 10_1^+$ level within both the full space (B) (dashed line left-hand scale) and the pure neutron two-hole $(1h_{11/2})^{-2}$ configuration (full line) as a function of the deexcitation gamma energy $E\gamma$. Both results for $e_n = 0.5e$ (right-hand scale) and $1.0e$ (left-hand scale) are given.

could be provided through an $E2$ transition between levels of the almost pure $(1h_{11/2})_{10^+}^{-2}$ and $(1h_{11/2})_{8^+}^{-2}$ neutron configurations. Since the experimental $J^\pi = 10^+$ level is not known experimentally in a unique way, an upper limit could, however, be deduced when associating the 3.9 μsec isomeric level with the $J_i^\pi = 10_1^+$ level[22] feeding the 2.701 keV $J_i^\pi = 8_1^+$ level with a low-energy transition. We have calculated for pure configurations

$$B(E2; 10_1^+ \to 8_1^+) = 68 |e_n^{\mathrm{eff}} \begin{Bmatrix} 10 & 8 & 2 \\ \frac{11}{2} & \frac{11}{2} & \frac{11}{2} \end{Bmatrix} \langle 1h_{11/2} \| r^2 Y_2 \| 1h_{11/2} \rangle|^2 ,$$

as well as for the exact diagonalization in the full space (B), the $T_{1/2}(10^+)$ value as a function of E_γ (see Fig. 6), taking into account the theoretical conversion coefficient $\alpha_K + \alpha_L + \alpha_M$ (Ref. 23). In this calculation, one observes that for $E_\gamma \simeq 50$ keV, half-lives of the desired order of magnitude occur and can explain the experimental half-life of a $J_i^\pi = 10_1^+$ level close to and above the $J_i^\pi = 8_1^+$ 2.701 MeV level in $^{134}_{52}\mathrm{Te}_{80}$. In the further deexciting mechanism, the $J_i^\pi = 8_1^+$ level will proceed via the $J_i^\pi = 6_1^+$ and 7_1^- levels. Half-lives for the corresponding transitions were calculated with as a result for particle half-lives $T_{1/2}$ (part.; $8_1^+ \to 6_1^+$) = 10 nsec (B) and $T_{1/2}$ (part.; $8_1^+ \to 7_1^-$) = 23.4 nsec (B). Therefore, one can conclude that within a

consistent microscopic calculation of the $^{132}_{52}Te_{80}$ level scheme, transition rates for some interesting low-lying levels as well as a recently discovered 3.9 μsec isomeric state[22] can qualitatively be accounted for, except for the $7_1^- \to 6_1^+ E1$ transition rate.

V. CONCLUSION

Starting from the recent experimental data on the $^{132}_{52}Te_{80}$ nucleus, it has become interesting to perform more refined shell-model calculations in order to explain both the proton and neutron excitations, clearly observable in the experimental data. We have pointed out that both a proton two-particle-(neutron two-hole-) core coupling calculation does not yield a satisfactory explanation for both types of excitations, i.e., the core excitations deviate too strongly from the underlying harmonic quadrupole assumption.

In a shell-model calculation treating both types of excitations (protons and neutrons) on equal footing and considering the p-p, n-n, and p-n interactions, it becomes possible to explain both the low-lying negative parity states $J_i^\pi = 7_1^-$, 5_1^- as neutron two-hole excitations and the $J_i^\pi = 4_1^+$, 6_1^+ levels as mainly proton two-particle excitations. Moreover, the p-n interaction results in being fairly weak in order to clearly establish these features. The problem of low-lying $J^\pi = 2^+$ states originating from the $|2_1^+(\nu)\otimes 0_1^+(\pi)\rangle$ configurations also can find a probable solution in the recently discovered low-lying 1.665 MeV (2^+) level, although the excitation energy of the 2_2^+ level is not reproduced correctly. The $J^\pi = (3,4)$ level at 2.107 MeV probably corresponds to the $|2_1^+(\nu)\otimes 2_1^+(\pi); 4^+\rangle$ configuration. Thereby, all important levels below $E_x < 2.1$ MeV find a simple explanation in terms of weak coupling of the $^{134}_{52}Te_{82}$ and $^{130}_{50}Sn_{80}$ nuclear systems, even if the excitation energies are not always reproduced correctly ($J^\pi = 2_{2,3}^+$ levels). The weak-coupling quintuplet $|2_1^+(\nu)\otimes 2_1^+(\pi); J^\pi\rangle$ has also been calculated although no clear experimental evidence for definitely locating these levels is available as yet. Concerning the electromagnetic transition probabilities, the half-life of the $J_i^\pi = 6_1^+$ level was reproduced as 257 nsec [226 nsec in full space (B)], a result that is still too slow compared with experiment. Also, no important $E1$ transitions can occur within the model space as considered here, therefore the μsec lifetime for the $J_i^\pi = 7_1^-$ level remains unexplained. A recently discovered isomeric level with $T_{1/2}(\text{expt.}) = 3.9$ μsec can find a probable explanation as a $J_i^\pi = 10_1^+$ level, feeding the underlying $J_i^\pi = 8_1^+$ level through a very low energy [< 50 keV] transition.

ACKNOWLEDGMENTS

The authors are much indebted to Professor A. J. Deruytter for his interest during the course of this work as well as to Dr. F. Schussler, Dr. K. Sistemich, Professor B. Walters, and Dr. R. A. Meyer for communicating results prior to publication. One of the authors (J.S.) is grateful to Professor A. J. Deruytter for financial support during his stay at the INW, Gent.

APPENDIX A

We first point out that the operators $A_\alpha^\dagger$ [see Eqs. (2.2) and (2.5)] stand for creation operators for particle or hole states, i.e., they are defined as follows:

$A_\alpha^\dagger \equiv a_\alpha^\dagger$ for particle excitations and

$A_\alpha^\dagger \equiv (-1)^{j_a + m_a} a_{a,-m_a}$ for hole excitations.

Here, we use the greek letter α for $\alpha \equiv \{a, m_a\}$. Also, the single-particle (-hole) energies E_a denote the positive quantities $E_a \equiv \epsilon_a$ for particle excitations and $E_a \equiv -\epsilon_a$ for hole excitations. These numbers are given in Table I. Whenever, in two-body matrix elements, the quantum numbers corresponding with hole configurations occur, we explicitly indicate if the hole configuration occurs as such by using the notation h^{-1}. Furthermore, to simplify the formulas, we use the following notation for the quantum numbers $\rho' \equiv (p', m_p')$, $\eta' \equiv (h', m_h')$, $\rho \equiv (\rho, m_p)$, $\eta \equiv (h, m_h)$, respectively.

We shall now derive the relation (2.6) from expression (2.5) and we also show the advantage of using the representation (2.5) for the particle-hole interaction. Usually, the particle-hole interaction can be expressed in terms of the two-body particle-hole matrix element $\langle p'h'^{-1}, J_1|V_{ph}|ph^{-1}, J_1\rangle$, i.e.,

$$V_{ph} = \sum_{\substack{\rho,\rho'\eta,\eta' \\ J_1,M_1}} \langle p'h'^{-1}, J_1|V_{ph}|ph^{-1}, J_1\rangle A_\rho^\dagger, A_\eta^\dagger, A_\eta A_\rho \langle j_p, m_{p'}, j_{h'}, m_{h'}|J_1 M_1\rangle \langle j_p m_p j_h m_h|J_1 M_1\rangle . \tag{A1}$$

The matrix elements of V_{ph} between the two-hole–two-particle wave functions of (2.2) result in a sum of

16 terms. The use of (A1) leads to the following expression for the quantity F of expression (2.6) (see also Ref. 24):

$$F(h_1'h_2'J_n',\ p_1'p_2'J_p';\ h_1h_2J_n,\ p_1p_2J_p;J) \equiv \hat{J}_p\hat{J}_p'\hat{J}_n\hat{J}_n'\,\delta_{h_1h_1'}\,\delta_{p_2p_2'}\,NN'$$
$$\times(-1)^{j_{p_1'}+j_{h_2'}+j_{p_1}+j_{h_2}+J_p+J_n+J_n'+J_p'}\sum_{J_1}\hat{J}_1^2\langle p_1'h_2'^{-1},J_1|V_{ph}|p_1h_2^{-1},J_1\rangle$$
$$\times\begin{bmatrix} J_n' & j_{p_1'} & J_n & j_{p_1}\\ J & j_{h_1} & j_{p_2} & J_1\\ J_p' & J_p & j_{h_2'} & j_{h_2}\end{bmatrix}. \qquad \text{(A2)}$$

The quantity between square brackets in the summation is a 12-j symbol of the second kind following the notation of Ref. 25, p.62. The 16 terms of the total matrix element can then be generated as indicated by relations (2.7) and (2.8). Let us now start from the expression (2.5),

$$V_{ph}=\sum_{\substack{\rho',\rho,\eta',\eta\\ J',M'}} U((p'p)(h'h);J')\,A_\rho^\dagger A_{\eta'}^\dagger A_\eta A_p\,(-1)^{j_p'-m_p'+j_h'-m_h'+J'-M'}\begin{pmatrix} j_p' & j_p & J'\\ -m_p' & m_p & -M'\end{pmatrix}\begin{pmatrix} j_h' & j_h & J'\\ -m_h' & m_h & M'\end{pmatrix}. \qquad \text{(A3)}$$

The quantities $U((p'p)(h'h);J')$, defined by the previous relation, can be calculated once for all and stored for computer calculations. Obviously, the $U((p'p)(h'h);J')$ and the $\langle p'h'^{-1},J_1|V_{ph}|ph^{-1},J_1\rangle$ are related. We obtain

$$U((p'p)(h'h);J')=\hat{J}'^2\sum_{J_1}\hat{J}_1^2(-1)^{j_p'+j_h+J'+J_1}\begin{Bmatrix} j_p' & J_1 & j_h'\\ j_h & J' & j_p\end{Bmatrix}\langle p'h'^{-1},J_1|V_{ph}|ph^{-1},J_1\rangle. \qquad \text{(A4)}$$

Using (2.5) or (A3) we can calculate the matrix element of V_{ph} between two-hole–two-particle wave functions. The quantity F of expression (2.6) can be written compactly using graphical methods for operations with sums of products of Wigner coefficients (Ref. 25, Chap. III) with, as a result,

$$F(h_1'h_2'J_n',\ p_1'p_2'J_p',\ h_1h_2J_n,\ p_1p_2J_p;J)\equiv\hat{J}_p'\hat{J}_n'\hat{J}_p\hat{J}_n\,\delta_{h_1h_1'}\,\delta_{p_2p_2'}\,NN'\sum_{J'}U((p_1'p_1)(h_2'h_2);J')\,\mathcal{G}, \qquad \text{(A5)}$$

where $\mathcal{G}$ is the diagram of Fig. 7. This diagram is the product of three 6-j symbols and a phase factor, since it is easily separable (see Ref. 25; pp.47 and 50). The separation lines are shown by dashed lines in Fig. 7. Then formula (2.6) follows immediately as

$$F(h_1'h_2'J_n',\ p_1'p_2'J_p';\ h_1h_2J_n,\ p_1p_2J_p;J)\equiv\hat{J}_p\hat{J}_n\hat{J}_p'\hat{J}_n'\,\delta_{h_1h_1'}\,\delta_{p_2p_2'}\,NN'$$
$$\times\sum_{J'}U((p_1'p_1)(h_2'h_2);J')\begin{Bmatrix} j_{h_2'} & J' & j_{h_2}\\ J_n & j_{h_1} & J_n'\end{Bmatrix}\begin{Bmatrix} J_p & J' & J_p'\\ J_n' & J & J_n\end{Bmatrix}\begin{Bmatrix} J_p & J' & J_p'\\ j_{p_1'} & j_{p_2} & j_{p_1}\end{Bmatrix}$$
$$\times(-1)^{j_{h_1}+J_p+J+J_n+J'+J_n'+j_{p_1}+J_p'+j_{p_2}+j_{h_2'}}. \qquad \text{(A6)}$$

From a computational point of view, we have only to deal with a product of three 6-j symbols instead of a 12-j symbol of the second kind as was the case in (A2). In the former case, much less time is needed for the calculation of the two-hole–two-particle matrix elements.

One can now easily prove the equivalence of (A6) and (A2) by substituting the explicit form of the U-matrix elements (A4) into (A6) and using relation (19.3) of Ref. 25 giving the summation over four 6-j symbols as a 12-j symbol of the second kind.

APPENDIX B

Here, we shall derive the reduced transition matrix element. The transition operator consists of an operator acting in neutron space $\Omega_\lambda(n)$ and an operator acting in proton space $\Omega_\lambda(p)$. We deal first with the

proton operator. Using relation (15.27) of Ref. 26, one gets

$$\Omega_p(h_1' h_2' J_n', p_1' p_2' J_p', J_f, h_1 h_2 J_n, p_1 p_2 J_p, J_i)$$

$$\equiv \hat{J}_i \hat{J}_f \delta_{J_n J_n'} D(h_1' h_2', h_1 h_2; J_n)[(1+\delta_{h_1 h_2})(1+\delta_{h_1' h_2'})]^{-1/2}(-1)^{J_n + J_p + J_f + \lambda}$$

$$\times \langle p_1' p_2', J_p' \| \Omega_\lambda \| p_1 p_2, J_p \rangle \begin{Bmatrix} J_p' & \lambda & J_p \\ J_i & J_n & J_f \end{Bmatrix} . \tag{B1}$$

The proton reduced matrix elements is the sum of four terms. One of them is, always using relation (15.27) of Ref. 26.

$$\mathfrak{M}_p \equiv \delta_{p_1 p_1'}(-1)^{j_{p_1} + j_{p_2} + J_p' + \lambda} \hat{J}_p \hat{J}_p' [(1+\delta_{p_1 p_2})(1+\delta_{p_1' p_2'})]^{-1/2}$$

$$\times \begin{Bmatrix} j_{p_2'} & \lambda & j_{p_2} \\ J_p & j_{p_1} & J_p' \end{Bmatrix} \langle p_2' \| \Omega_\lambda \| p_2 \rangle . \tag{B2}$$

We can use (B2) and (B1) to obtain the relation (3.2)

$$\Omega_p(h_1' h_2' J_n', p_1' p_2' J_p', J_f; h_1 h_2 J_n, p_1 p_2 J_p, J_i) \equiv \hat{J}_i \hat{J}_f \hat{J}_p \hat{J}_p' \delta_{J_n J_n'} \delta_{p_1 p_1'} D(h_1' h_2', h_1 h_2; J_n) NN' (-1)^{j_{p_1} + j_{p_2} + J_p + J_n + J_p' + J_f}$$

$$\times \begin{Bmatrix} J_p' & \lambda & J_p \\ J_i & J_n & J_f \end{Bmatrix} \begin{Bmatrix} j_{p_2'} & \lambda & j_{p_2} \\ J_p & j_{p_1} & J_p' \end{Bmatrix} \langle p_2' \| \Omega_\lambda \| p_2 \rangle . \tag{B3}$$

The relation (3.3) then generates the four terms of the proton contribution. The neutron contribution is also the sum of four terms which are obtained in the same way. Making use of relation (15.26) of Ref. 26, we have first

$$\Omega_n(h_1' h_2' J_n', p_1' p_2' J_p', J_f; h_1 h_2 J_n, p_1 p_2 J_p, J_i)$$

$$\equiv \hat{J}_i \hat{J}_f \delta_{J_p J_p'} D(p_1' p_2', p_1 p_2; J_p)[(1+\delta_{p_1 p_2})(1+\delta_{p_1' p_2'})]^{-1/2}(-1)^{J_n' + J_p + J_i + \lambda}$$

$$\times \begin{Bmatrix} J_n' & \lambda & J_n \\ J_i & J_p & J_f \end{Bmatrix} \langle h_1' h_2', J_n' \| \Omega_\lambda \| h_1 h_2, J_n \rangle . \tag{B4}$$

One of the terms of the reduced neutron matrix element, using (15.27) of Ref. 26, and also taking into account that the neutron states are hole states, is obtained as

$$\mathfrak{M}_n \equiv \delta_{h_1 h_1'}(-1)^{J_n' + j_{h_2'}} (-1)^{j_{h_1}} [(1+\delta_{h_1 h_2})(1+\delta_{h_1' h_2'})]^{-1/2} \hat{J}_n \hat{J}_n' \begin{Bmatrix} j_{h_2}' & \lambda & j_{h_2} \\ J_n & j_{h_1} & J_n' \end{Bmatrix} \langle h_2 \| \Omega_\lambda \| h_2' \rangle . \tag{B5}$$

Combining now (B4) and (B5), expression (3.4) is obtained,

$$\Omega_n(h_1' h_2' J_n', p_1' p_2' J_p', J_f; h_1 h_2 J_n, p_1 p_2 J_p, J_i) \equiv \hat{J}_i \hat{J}_f \hat{J}_n \hat{J}_n' \delta_{J_p J_p'} \delta_{h_1 h_1'} D(p_1' p_2', p_1 p_2; J_p) NN' (-1)^{J_p + J_i + j_{h_2'} - j_{h_1} + \lambda}$$

$$\times \begin{Bmatrix} J_n' & \lambda & J_n \\ J_i & J_p & J_f \end{Bmatrix} \begin{Bmatrix} j_{h_2'} & \lambda & j_{h_2} \\ J_n & j_{h_1} & J_n' \end{Bmatrix} \langle h_2 \| \Omega_\lambda \| h_2' \rangle . \tag{B6}$$

Then the four terms of the neutron contribution are generated in the same way as in the proton case.

APPENDIX C

Rewriting the residual interaction Hamiltonian of Eq. (2.1) that acts in the one particle-one hole space, one obtains, specializing to the notation of Appendix A, the following expression for V_{ph},

$$V_{ph} = 4 \sum_{\rho, \rho', \eta, \eta'} s_\eta s_{\eta'} V'_{\rho' \bar{\eta} \bar{\eta}' \rho} A^\dagger_{\rho'} A^\dagger_{\eta'} A_\eta A_\rho . \tag{C1}$$

Here, we use the notation $\bar{\rho} \equiv (p, -m_p)$, etc., and moreover, use the definition of $s_\rho \equiv (-1)^{j_p - m_p}$

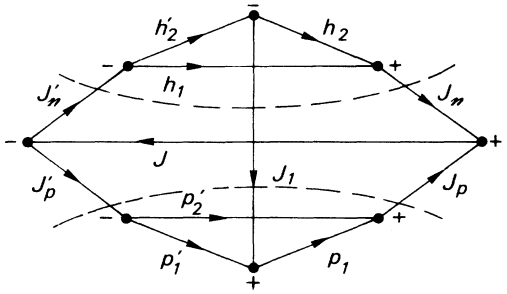

FIG. 7. The summation of 3-j symbols, resulting in Eq. (A6), carried out in a graphical way.

in order to simplify the expressions. We can now, as shown by Baranger,[27] use three different methods of vector coupling the V' matrix elements:

(i) Using the standard particle-particle coupling of angular momentum, i.e., $(\rho', \bar{\eta})$ and $(\bar{\eta}', \rho)$, one obtains

$$V'_{\rho'\bar{\eta}\bar{\eta}'\rho} = -\tfrac{1}{2}\sum_{J,M} G(p'h, h'p; J) \times\langle j'_p m'_p, j_h - m_h | JM\rangle \times\langle j'_h - m'_h, j_p m_p | JM\rangle , \quad \text{(C2)}$$

and then the resulting particle-hole interaction reads

$$V_{ph} = -2\sum_{\substack{\rho,\rho',\eta,\eta' \\ J,M}} s_\eta s_{\eta'} G(p'h, h'p; J) \times\langle j'_p m'_p, j_h - m_h | JM\rangle \times\langle j'_h - m'_h, j_p m_p | JM\rangle \times A^\dagger_{\rho'} A^\dagger_{\eta'} A_\eta A_\rho . \quad \text{(C3)}$$

(ii) Using the angular momentum coupling scheme $(\rho', \bar{\eta}')$ and $(\rho, \bar{\eta})$. According to Ref. 27, one obtains

$$V'_{\rho'\bar{\eta}\bar{\eta}'\rho} = -\tfrac{1}{2}\sum_{J,M} F(p'h', ph; J)\langle j'_p m'_p, j'_h m'_h | JM\rangle \times j_p m_p, j_h m_h | JM\rangle\, s_{\bar{\eta}}\, s_{\bar{\eta}'} , \quad \text{(C4)}$$

and the interaction V_{ph} becomes

$$V_{ph} = -2\sum_{\substack{\rho,\rho',\eta,\eta' \\ J,M}} F(p'h', ph; J)\langle j'_p m'_p, j'_h m'_h | JM\rangle \times\langle j_p m_p, j_h m_h | JM\rangle A^\dagger_{\rho'} A^\dagger_{\eta'} A_\eta A_\rho , \quad \text{(C5)}$$

being equal to our expression (A1) since $-2F(p'h', ph; J)$ is equal to $\langle p'h'^{-1}, J | V | ph^{-1}, J\rangle$ (Ref. 28).

(iii) Using a third angular momentum coupling scheme for (ρ', ρ) and $(\bar{\eta}', \bar{\eta})$, again using Ref. 27, one obtains

$$V'_{\rho'\bar{\eta}\bar{\eta}'\rho} = \tfrac{1}{2}\sum_{J,M} F(p'p, h'h; J) s_\rho s_{\bar{\eta}} \times\langle j'_p m'_p, j_p - m_p | JM\rangle \times\langle j'_h - m'_h, j_h m_h | JM\rangle . \quad \text{(C6)}$$

Making use of the symmetry relations for the F-matrix elements and using 3-j symbols we obtain for V_{ph} the resulting expression

$$V_{ph} = 2\sum_{\substack{\rho,\rho',\eta,\eta' \\ J,M}} F(pp', hh'; J)(2J+1) \times\begin{pmatrix} j'_p & j_p & J \\ -m'_p & m_p & -M \end{pmatrix}\begin{pmatrix} j'_h & j_h & J \\ -m'_h & m_h & M \end{pmatrix} \times s_{\rho'} s_{\eta'} (-1)^{J-M} A^\dagger_{\rho'} A^\dagger_{\eta'} A_\eta A_\rho . \quad \text{(C7)}$$

Then, a relation with our U-matrix elements results in

$$U(p'p, h'h; J) = 2F(pp', hh'; J)(2J+1), \quad \text{(C8)}$$

thus one also has

$$U(p'p, h'h; J) = -(2J+1)\langle pp'^{-1}, J | V | hh'^{-1}, J\rangle . \quad \text{(C9)}$$

Next to Eq. (A4), one can also give the relation with the usual particle-particle coupled matrix elements as

$$U(p'p, h'h; J) = -(2J+1)\sum_{J'}(2J'+1)(-1)^{j'_p + j_h + J'}\begin{Bmatrix} j'_p & j_p & J \\ j'_h & j_h & J' \end{Bmatrix} \times\langle p'h, J' | V | ph', J'\rangle . \quad \text{(C10)}$$

APPENDIX D

Here, we would like to prove explicitly the equivalence of our expressions (2.6) and (2.8) with the two-particle-two-hole matrix element as given by Ma and True[24] in their Eqs. 5 and 6. Taking the expression (2.6), and filling into it the relation (C10), relating the U-matrix element with the particle-particle coupled matrix element, one gets

$$-\sum_{J',J''}(2J'+1)(2J''+1)\langle p_1' h_2, J''|V|p_1 h_2', J''\rangle \begin{Bmatrix} j'_{h_2} & J' & j_{h_2} \\ J_n & j_{h_1} & J'_n \end{Bmatrix}\begin{Bmatrix} J_p & J' & J'_p \\ J'_n & J & J_n \end{Bmatrix}$$

$$\times \begin{Bmatrix} J_p & J' & J'_p \\ j'_{p_1} & j_{p_2} & j_{p_1} \end{Bmatrix}\begin{Bmatrix} j'_{p_1} & j_{p_1} & J' \\ j'_{h_2} & j_{h_2} & J'' \end{Bmatrix}\delta_{h_1 h_1'}\,\delta_{p_2 p_2'}(-1)^{j'_{p_1}+j_{h_2}+j_{h_1}+j_{p_1}+j_{p_2}+j'_{h_2}+J''+J_p+J+J_n+J'+J'_n+J'_p}\,. \tag{D1}$$

We then also get, after reordering the 6-j symbols, the expression

$$-\sum_{J''}(2J''+1)\Big[\sum_{J'}(2J'+1)\begin{Bmatrix} J'_p & J_p & J' \\ J_n & J'_n & J \end{Bmatrix}\begin{Bmatrix} J'_n & J_n & J' \\ j_{h_2} & j'_{h_2} & j_{h_1} \end{Bmatrix}\begin{Bmatrix} j'_{h_2} & j_{h_2} & J' \\ j'_{p_1} & j_{p_1} & J'' \end{Bmatrix}\begin{Bmatrix} j_{p_1} & j'_{p_1} & J' \\ J'_p & J_p & j_{p_2} \end{Bmatrix}(-1)^{\text{phase}+J'}\Big]$$

$$\times\langle p_1' h_2, J''|V|p_1 h_2', J''\rangle\,\delta_{h_1 h_1'}\,\delta_{p_2 p_2'}\,, \tag{D2}$$

[calling $(-1)^{\text{phase}+J'}=(-1)^{j'_{p_1}+\cdots+J'_p}$ of Eq. (D1)].

Applying now, Eq. (19.1) of Yutsis *et al.* (Ref. 25), one easily gets

$$-\sum_{J''}(2J''+1)\begin{Bmatrix} J'_p & J'_n & j'_{h_2} & j_{p_1} \\ J & j_{h_1} & J'' & j_{p_2} \\ J_p & J_n & j_{h_2} & j'_{p_1} \end{Bmatrix}\langle p_1' h_2, J''|V|p_1 h_2', J''\rangle\,\delta_{h_1 h_1'}\,\delta_{p_2 p_2'}\,, \tag{D3}$$

obtaining a 12-j symbol of the first kind. In these expressions [(D1) to (D3)], we left aside, and will do so further on, the norm NN' as well as the factor $\hat{J}_p\hat{J}'_p\hat{J}_n\hat{J}'_n$.

Now, the result (D3) has been obtained starting from the two-hole–two-particle configuration, denoted as

$$\langle (h_1' h_2')J'_n(p_1' p_2')J'_p, J|V|(h_1 h_2)J_n(p_1 p_2)J_p, J\rangle\,, \tag{D4}$$

and calculating our first term as (D3). Conforming to the notation of Ma and True[24] (for the analogous matrix element) in calculating

$$\langle (H_1 H_2)J_1(P_1 P_2)J_2, J|V|(H_3 H_4)J_3(P_3 P_4)J_4, J\rangle\,, \tag{D5}$$

this corresponds to the 7th term of Ma and True's Eq. (6), giving after some reordering the resulting contribution of

$$-\sum_{J''}(2J''+1)\begin{Bmatrix} P_2 & P_3 & J_4 & J_3 \\ P_1 & J'' & H_4 & J_1 \\ J_2 & H_2 & J & H_1 \end{Bmatrix}\langle P_1 H_4, J''|V|P_3 H_2, J''\rangle\,\delta_{H_1 H_3}\,\delta_{P_2 P_4}\,. \tag{D6}$$

If we now make the substitution of corresponding quantum numbers from (D4) and (D5), one gets the result

$$-\sum_{J''}(2J''+1)\begin{Bmatrix} j_{p_2} & j_{p_1} & J_p & J_n \\ j'_{p_1} & J'' & j_{h_2} & J'_n \\ J'_p & j'_{h_2} & J & j_{h_1} \end{Bmatrix}\langle p_1' h_2, J''|V|p_1 h_2', J''\rangle\,\delta_{h_1 h_1'}\,\delta_{p_2 p_2'}\,. \tag{D7}$$

This points already to the equivalence of (D7) and (D3), since the 12-j symbol defined according to Rotenberg [see Eq. (A1) of Ma and True, Ref. 24], is also a 12-j symbol of the first kind (the notation of Rotenberg, however, differs from Yutsis *et al.*[25]). This can be seen explicitly from the equation (A1) of Ref. 24, since

$$\begin{Bmatrix} j_{p_2} & j_{p_1} & J_p & J_n \\ j'_{p_1} & J'' & j_{h_2} & J'_n \\ J'_p & j'_{h_2} & J & j_{h_1} \end{Bmatrix}=\sum_{J'}\begin{Bmatrix} j_{p_1} & j'_{p_1} & J' \\ J'_p & J_p & j_{p_2} \end{Bmatrix}\begin{Bmatrix} J'_p & J_p & J' \\ J_n & J'_n & J \end{Bmatrix}\begin{Bmatrix} J_n & J'_n & J' \\ j'_{h_2} & j_{h_2} & j_{h_1} \end{Bmatrix}\begin{Bmatrix} j'_{h_2} & j_{h_2} & J' \\ j'_{p_1} & j_{p_1} & J'' \end{Bmatrix}(2J'+1)\,(-1)^{\text{phase}+J'}\,, \tag{D8}$$

a definition that exactly corresponds to the one as used in (D2). Thereby, we have proven the complete equivalence of our Eq. (2.8) and Eq. (6) of Ref. 24.

*Permanent address: Institut de Physique Nucléaire and IN2P3, Université Claude Bernard, Lyon-1 43, Bd du 11 Novembre 1918-69622 Villeurbanne-Cedex, France.

[1]B. Fogelberg, P. Carlé, and T. Nagarajan, annual report, Research Inst. of Physics, Stockholm, 84 (1976).
[2]E. Lund, K. Aleklett, and G. Rudstam, Nucl. Phys. A286, 403 (1977).
[3]E. A. Henry, S. M. Lane, and R. A. Meyer, Bull. Am. Phys. Soc. 22, 1031 (1977).
[4]A. Kerek, P. Carlé, and S. Borg, Nucl. Phys. A224, 367 (1974).
[5]J. McDonald and A. Kerek, Nucl. Phys. A206, 417 (1973).
[6]F. Schussler, private communication.
[7]E. Degrieck and G. Vanden Berghe, Nucl. Phys. A231, 141 (1974).
[8]E. Degrieck and G. Vanden Berghe, Z. Phys. 265, 393 (1973).
[9]A. Kerek, G. B. Holm, S. Borg, and L. E. De Geer, Nucl. Phys. A195, 177 (1972).
[10]R. A. Meyer, O. G. Lien, E. A. Henry, and S. M. Lane, Bull. Am. Phys. Soc. 22, 1243 (1977).
[11]A. Kerek, G. B. Holm, S. Borg, and P. Carlé, Nucl. Phys. A209, 520 (1973).
[12]A. Kerek, G. B. Holm, P. Carlé, and J. McDonald, Nucl. Phys. A195, 159 (1972).
[13]M. Waroquier and K. Heyde, Nucl. Phys. A164, 113 (1971).
[14]K. Heyde and M. Waroquier, Nucl. Phys. A167, 545 (1971).
[15]M. Waroquier and K. Heyde, Z. Phys. 268, 11 (1974).
[16]P. Van Isacker, K. Heyde, M. Waroquier, and H. Vincx, Phys. Rev. C 19, 498 (1979).
[17]K. Heyde, J. Sau, R. Chery, F. Schussler, J. Blachot, J. P. Bocquet, E. Monnand, and K. Sistemich, Phys. Rev. C 16, 2437 (1977).
[18]K. Sistemich, W. D. Lauppe, H. Lawin, F. Schussler, J. P. Bocquet, E. Monnand, and J. Blomqvist, Z. Phys. A292, 145 (1979).
[19]P. Kleinheinz, private communication.
[20]A. Bohr and B. Mottelson, *Nuclear Structure* (Benjamin, New York, 1975), Vol. 2.
[21]G. Alaga, in *Nuclear Structure and Nuclear Reactions*, edited by M. Jean and R. A. Ricci (Academic, New York, 1969).
[22]K. Sistemich, private communication (unpublished).
[23]R. S. Hager and E. C. Seltzer, Nucl. Data A4, 1 (1968).
[24]W. W. True and C. W. Ma, Phys. Rev. C 9, 2275 (1974).
[25]A. P. Yutsis, I. B. Levinson, and V. V. Vanagas, *Angular Momentum* (Israel Program for Scientific Translation, Jerusalem, 1962).
[26]I. Talmi and A. De Shalit, *Nuclear Shell Theory* (Academic, New York, 1963).
[27]M. Baranger, Phys. Rev. 120, 957 (1960).
[28]T. T. S. Kuo, E. U. Baranger, and M. Baranger, Nucl. Phys. 79, 513 (1966).